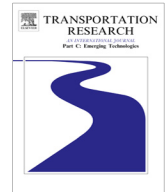




ELSEVIER

Contents lists available at ScienceDirect

# Transportation Research Part C

journal homepage: [www.elsevier.com/locate/trc](http://www.elsevier.com/locate/trc)

## Highway traffic state estimation with mixed connected and conventional vehicles: Microscopic simulation-based testing <sup>☆</sup>



Markos Fountoulakis <sup>a,\*</sup>, Nikolaos Bekiaris-Liberis <sup>a</sup>, Claudio Roncoli <sup>b</sup>, Ioannis Papamichail <sup>a</sup>,  
Markos Papageorgiou <sup>a</sup>

<sup>a</sup> Dynamic Systems and Simulation Laboratory, Technical University of Crete, Chania 73100, Greece

<sup>b</sup> Department of Built Environment, School of Engineering, Aalto University, 02150 Espoo, Finland

### ARTICLE INFO

#### Article history:

Received 6 July 2016

Received in revised form 15 February 2017

Accepted 16 February 2017

Available online 7 March 2017

#### Keywords:

Traffic estimation

Connected vehicles

Microscopic simulation

### ABSTRACT

This paper presents a thorough microscopic simulation investigation of a recently proposed methodology for highway traffic estimation with mixed traffic, i.e., traffic comprising both connected and conventional vehicles, which employs only speed measurements stemming from connected vehicles and a limited number (sufficient to guarantee observability) of flow measurements from spot sensors. The estimation scheme is tested using the commercial traffic simulator Aimsun under various penetration rates of connected vehicles, employing a traffic scenario that features congested as well as free-flow conditions. The case of mixed traffic comprising conventional and connected vehicles equipped with adaptive cruise control, which feature a systematically different car-following behavior than regular vehicles, is also considered. In both cases, it is demonstrated that the estimation results are satisfactory, even for low penetration rates.

© 2017 Elsevier Ltd. All rights reserved.

## 1. Introduction

Traffic congestion is a significant problem for the majority of large cities in the modern world (Papageorgiou et al., 2007). While the number of vehicles has been increasing steadily during the past decades (Dargay et al., 2007), a corresponding expansion of road networks is not deemed feasible for various reasons. On the other hand, traffic management represents a valid alternative allowing to improve the performance of traffic systems with fairly moderate effort. For this reason, traffic authorities and automobile industries are currently focusing on the development of innovative methods for traffic monitoring (Bishop, 2005).

Real-time traffic state estimation utilizing limited traffic data is of major importance, not only for traffic monitoring but also for traffic control. In conventional traffic, real-time traffic data are provided by spot sensors positioned at appropriate locations on the highway. Since the cost of installation and maintenance of a sufficient number of spot sensors that guarantees accurate traffic monitoring is high, several studies deal with the development of traffic estimation algorithms employing a limited amount of sensors, such as, for example, Muñoz et al. (2003), Alvarez-Icaza et al. (2004), Wang and Papageorgiou (2005), Hegyi et al. (2006), Mihaylova et al. (2007), Morbidi et al. (2014), to name only a few.

<sup>☆</sup> This article belongs to the Virtual Special Issue on: "Management of Future Motorway and Urban Traffic Systems".

\* Corresponding author.

E-mail addresses: [mfountoul@dssl.tuc.gr](mailto:mfountoul@dssl.tuc.gr) (M. Fountoulakis), [nikos.bekiaris@dssl.tuc.gr](mailto:nikos.bekiaris@dssl.tuc.gr) (N. Bekiaris-Liberis), [claudio.roncoli@aalto.fi](mailto:claudio.roncoli@aalto.fi) (C. Roncoli), [ipapa@dssl.tuc.gr](mailto:ipapa@dssl.tuc.gr) (I. Papamichail), [markos@dssl.tuc.gr](mailto:markos@dssl.tuc.gr) (M. Papageorgiou).

The eminent need for improvement of traffic conditions, for enhancement of driver safety and comfort, and for reduced operation cost of traffic systems has led to the introduction of various Vehicle Automation and Communication Systems (VACS). VACS capabilities can be exploited for the development of novel traffic estimation and control methodologies (Diakaki et al., 2015). Traffic control in the presence of VACS is the subject of numerous papers, such as, for example, Varaiya (1993), Rao and Varaiya (1994), Rajamani and Shladover (2001), Bose and Ioannou (2003), Kesting et al. (2008), Shladover et al. (2012), Ge and Orosz (2014), Wang et al. (2014), Roncoli et al. (2015, 2016).

The problem of traffic estimation in the presence of VACS is addressed in numerous studies, such as, for example, Work et al. (2008), De Fabritiis et al. (2008), Herrera et al. (2010), Rahmani et al. (2010), Treiber et al. (2011), Gayah and Dixit (2013), Yuan et al. (2012), Ramezani and Geroliminis (2012), Yuan et al. (2014), Piccoli et al. (2015), Seo et al. (2015), Bekiaris-Liberis et al. (2016), Roncoli et al. (in press) to name only a few. Note that in Yuan et al. (2012, 2014) an extended Kalman filter that utilizes both Eulerian and Lagrangian measurements is employed, based on the Lagrangian coordinates model (where state variables move with the traffic stream) proposed by Leclercq et al. (2007). Typically, such traffic state estimation algorithms employ data stemming from connected vehicles, i.e., vehicles that can provide real-time information to a central or local authority (Turksma, 2000). Connected vehicle data can be utilized as a low-cost and efficient, complementary or primary, source of traffic information towards traffic state estimation (Treiber and Kesting, 2013).

In addition to vehicle communication systems, automated vehicle systems play an important role in modern intelligent transportation systems. While fully automated highways, an innovation that would affect traffic conditions significantly (Kesting et al., 2007), are unlikely to come into existence in the near future, partially automated highways are already part of reality. One of the crucial components of such automated systems is Adaptive Cruise Control (ACC), which was already introduced into modern vehicles by the automobile industry (Darbha and Rajagopal, 1999; Wang et al., 2014). ACC-equipped vehicles aim at increased driver safety and improved comfort (Dragutinovic et al., 2005) and may have a different car-following behavior than manually driven cars, thus changing the traffic flow characteristics accordingly. Since a high penetration rate of ACC-equipped vehicles is not yet a reality, the effect of various percentages of such vehicles on traffic conditions is typically examined utilizing microscopic simulation platforms, see, e.g., Treiber and Helbing (2001), Marsden et al. (2001), VanderWerf et al. (2001), Rajamani et al. (2005), van Arem et al. (2006), Kesting et al. (2007), Ntousakis et al. (2015).

In this paper, we continue and extend our research on the validation of the scheme developed in Bekiaris-Liberis et al. (2016) for estimation of densities and ramp flows, which is based on a simple but exact macroscopic model for traffic density and employs mainly speed measurements obtained from connected vehicles (equipped with ACC or not). The distinguishing characteristic of this estimation scheme, compared to virtually all previous related developments, is that it is only based on the conservation-of-vehicles equation, without the resort of fundamental diagrams or other empirical relationships, which would call for appropriate and tedious model validation procedures, before field application. We test the performance of the estimation scheme under mixed traffic conditions, where connected vehicles, equipped with ACC or not, are present at various penetration rates. We utilize for our testing the microscopic simulation software Aimsun (Transport Simulation Systems, 2014) in which we build a highway stretch that includes several on-ramps and off-ramps, and employ a scenario in which both congested and free-flow traffic conditions occur. We also evaluate the performance of the estimation scheme when, for some instances, a very limited (or literally zero) number of speed measurements from connected vehicles are available, and propose simple algorithms for resolving the problem of lack of reliable segment speed measurements. Moreover, it is demonstrated that density estimation is highly insensitive to the choice of the filter parameters, while ramp flow estimation is more sensitive.

The rest of the paper is structured as follows. Section 2 presents the estimation scheme employed. Section 3 describes the details of the microscopic simulation configuration as well as the traffic network and scenario employed. Section 4 presents the results of the estimation in mixed traffic, i.e., traffic comprising conventional and connected vehicles. Section 5 presents the results of the estimation in mixed traffic comprising conventional and ACC-equipped connected vehicles. Finally, Section 6 concludes the paper.

## 2. Traffic state estimation exploiting VACS capabilities

### 2.1. Innovative features of VACS

#### 2.1.1. Connected vehicles

Data stemming from connected vehicles may contain a wide variety of traffic information, but the most commonly used are vehicle position (longitude, latitude, and altitude) and vehicle speed. The most popular way of acquiring a vehicle's position is via the Global Positioning Systems (GPS), see, e.g., De Fabritiis et al. (2008), Rahmani et al. (2010), Herrera et al. (2010), although cellular positioning is also utilized, usually with less accurate results, see, e.g., Yim and Cayford (2001), Bar-Gera (2007). GPS is a low-cost, efficient solution to gather traffic data, with a reported position error of 5–15 m in older studies (Zito et al., 1995; Turksma, 2000), whereas recently, with the employment of Differential GPS (DGPS) and map-matching algorithms, position accuracy up to 1–5 m can be achieved (Waterson and Box, 2012). Speed measurement error is mostly reported to be as low as 1 km/h (Zito et al., 1995), reaching 5 km/h in some studies (Zhao et al., 2011). Data from connected vehicles are mainly transmitted to a central traffic authority, which reflects the so called Vehicle to Infrastructure (V2I) com-

munication, typically via a GPRS/GSM network (Bishop, 2005). In parallel, vehicles can send data to one another, via Vehicle to Vehicle (V2V) communication, usually utilizing WiFi 802.11 (Waterson and Box, 2012). Connected vehicle data are usually small in size, thus low-delay transmissions are possible (Messelodi et al., 2009). Reporting periods vary among different experiments and commercial systems, most frequently ranging between a few seconds and a few minutes, see, e.g., Bishop (2005), Zhang et al. (2007), Messelodi et al. (2009), Herrera et al. (2010).

### 2.1.2. Automated vehicles

As part of the Advanced Driver Assistance Systems (ADAS), earlier cruise control systems were designed to merely maintain a certain speed set by the driver. However, novel ACC systems are able, additionally to the cruise control feature, to preserve a predefined safety time-gap to the leading vehicle (Bishop, 2005). Usually, the desired ACC time-gap ranges between 0.9 and 2.5 s (Kesting et al., 2007), but might go as low as 0.5 s (van Arem et al., 2006). The objective of the ACC system is to compute and apply the appropriate acceleration or deceleration according to the driver settings and the surrounding conditions. In order for this to happen, information about the vehicle ahead is required, more specifically, the distance (space gap) and speed difference of the two vehicles, which can be obtained via on-board sensors (Kesting et al., 2007). Using this information, the ACC system calculates the necessary acceleration or deceleration and transforms it to actual throttling or breaking commands. Since the ACC system acquires knowledge of the preceding vehicle's position and speed (e.g., by measuring via on-board sensors the spacing and relative speed with respect to the preceding vehicle as well as its own position and speed), this information could be used to enhance the traffic information reported by an ACC-equipped connected vehicle, thus providing two speed measurements to the central authority instead of one. For more information on available ACC models and technologies, see, e.g., Bishop (2005), Rajamani et al. (2005), Diakaki et al. (2015), Ntousakis et al. (2015).

## 2.2. Traffic estimation using average speed measurements

### 2.2.1. Traffic density dynamics as an LPV system

We subdivide the highway into segments (e.g. of some 500 m in length) and consider the density  $\rho_i(k)$  of highway segment  $i$  at time step  $k$  to be the number of vehicles in the segment divided by the segment length  $\Delta_i$ . The dynamics of the density can be described by the following discrete-time equations

$$\rho_i(k+1) = \rho_i(k) + \frac{T}{\Delta_i} (q_{i-1}(k) - q_i(k) + r_i(k) - s_i(k)), \quad (1)$$

where  $i = 1, \dots, N$  is the index of the specific highway segment of the network,  $N$  being the number of segments on the highway,  $k$  is the discrete time index,  $\Delta_i$  is the length of segment  $i$  (km),  $q_i$  is the flow (veh/h) at the end of segment  $i$ , and  $T$  is the time-discretization step (h);  $r_i$  and  $s_i$  are the vehicle inflow and outflow (veh/h) at on-ramps and off-ramps included in the upstream part of the specific segment, respectively. Typically, a highway segment can contain no more than one ramp in total (either an on-ramp or an off-ramp). Given that

$$q_i(k) = \rho_i(k)v_i(k), \quad (2)$$

where  $v_i(k)$  is the average vehicle speed of segment  $i$  at time  $k$ , we can rewrite (1) as<sup>1</sup>

$$\rho_i(k+1) = \frac{T}{\Delta_i} v_{i-1}(k) \rho_{i-1}(k) + \left(1 - \frac{T}{\Delta_i} v_i(k)\right) \rho_i(k) + \frac{T}{\Delta_i} (r_i(k) - s_i(k)). \quad (3)$$

In order for the discrete-time relations (2) and (3) to be sufficiently accurate, the following inequality must hold

$$\max_{i,k} \frac{T}{\Delta_i} v_i(k) < 1. \quad (4)$$

As it is common practice in estimation applications while addressing unknown quantities (see, e.g., Wang and Papageorgiou (2005)), we assume that any unmeasured on-ramp and off-ramp flows are constant, or, effectively, slowly varying, so that the unmeasured ramp flow dynamics may be reflected by a random walk, i.e.,

$$\theta_i(k+1) = \theta_i(k) + \zeta_i^0(k), \quad (5)$$

where  $\zeta_i^0$  is zero-mean white Gaussian noise and

$$\theta_i = \begin{cases} \frac{T}{\Delta_i} r_{n_i}, & \text{if } n_i \in L_r \\ \frac{T}{\Delta_i} s_{n_i}, & \text{if } n_i \in L_s \end{cases}, \quad (6)$$

<sup>1</sup> Formula (2) may not be exact, but was found in according tests to be the most accurate simple (non-switching) modeling approach for flows. Note, however, that the corresponding error is accounted for in the estimation model via additive process and measurement noise.

for all  $i = 1, \dots, l_r + l_s$ . We consider  $L_r = \{n_1, \dots, n_{l_r}\}$  and  $L_s = \{n_{l_r+1}, \dots, n_{l_r+l_s}\}$  to be the sets of segments, denoted by  $n_i$ , which have an on-ramp or an off-ramp, respectively, whose flows are not directly measured. Moreover,  $l_r$  and  $l_s$  are the numbers of unmeasured on-ramp flows and off-ramp flows, respectively. Note that, since segments are specified such that they may contain either no ramp at all or one ramp in total, which may be an on-ramp or an off-ramp, there can be no more than one ramp (either an on-ramp or an off-ramp) with unmeasured flow in a segment.

Assuming that the average speed of conventional vehicles is roughly equal to the average speed of connected vehicles, and hence it is available with the traffic authority, one can consider that  $v_i, i = 1, \dots, N$ , are measured. Therefore, defining the state

$$x = (\rho_1, \dots, \rho_N, \theta_1, \dots, \theta_{l_r+l_s})^T, \quad (7)$$

the deterministic part of the dynamics of segment densities given in (3) and of  $\theta_i$  given in (5) can be written in the form of a Linear Parameter-Varying (LPV) system as

$$x(k+1) = A(v(k))x(k) + Bu(k), \quad (8)$$

where

$$A(v(k)) = \begin{cases} a_{ij} = \frac{T}{\Delta_i} v_{i-1}(k), & \text{if } i-j = 1 \text{ and } i \geq 2 \\ a_{ij} = 1 - \frac{T}{\Delta_i} v_i(k), & \text{if } i = j \\ a_{n_j} = 1, & \text{if } n_i \in L_r \text{ and } j = N + i \\ a_{n_j} = -1, & \text{if } n_i \in L_s \text{ and } j = N + i \\ a_{ij} = 1, & \text{if } N < i \leq N_1 \text{ and } j = i \\ a_{ij} = 0, & \text{otherwise} \end{cases} \quad (9)$$

$$B = \begin{cases} b_{ij} = \frac{T}{\Delta_i}, & \text{if } i = 1 \text{ and } j = 1 \\ b_{m_j} = \frac{T}{\Delta_{m_j}}, & \text{if } m_i \notin \bar{L}, 1 \leq m_i \leq N, 1 \leq i \leq N_2, \text{ and } j = i + 1 \\ b_{ij} = 0, & \text{otherwise} \end{cases} \quad (10)$$

$$u(k) = \begin{cases} u_i = q_0(k), & \text{if } i = 1 \\ u_{i+1} = r_{m_i} - s_{m_i}, & \text{if } m_i \notin \bar{L} \end{cases} \quad (11)$$

with  $\bar{L} = L_r \cup L_s$  being the set of segments which have an on-ramp or an off-ramp whose flows are not directly measured,  $N_1 = N + l_r + l_s, N_2 = N - l_r - l_s, A \in \mathbb{R}^{N_1 \times N_1}, B \in \mathbb{R}^{N_1 \times (N_2+1)}$ . We denote with  $m_i$  the segment where the  $i$ -th measured ramp is positioned and thus, entries of  $B$  matrix that correspond to a measured ramp are set equal to  $\frac{T}{\Delta_{m_i}}$  if  $j = i + 1$ . Note that  $q_0$  is the total flow of vehicles at the entry of the considered highway stretch and acts as a measured input to (8); along with any directly measured on-ramp and off-ramp flows,  $r_i$  and  $s_i, i \notin L_r, i \notin L_s$ , respectively; while  $v_i, i = 1, \dots, N$ , are viewed as time-varying parameters of (8). LPV systems are a well-studied subclass of linear time-varying systems, whose dynamics vary as a result of the variation of certain parameters.

Regarding the measured outputs, we assume that the flow at the mainstream exit of the highway, namely  $q_N$ , is available via a fixed flow detector, hence, the last segment's density can be computed as

$$\rho_N = \frac{q_N}{v_N}, \quad (12)$$

where  $v_N$  is the speed of the last segment, as reported by connected vehicles, and be used as a system output.

If there is exactly one unmeasured ramp within the considered highway stretch, then no additional measurements are necessary for flow observability. On the other hand, if there are more than one unmeasured ramps within the stretch, we need (for flow observability) one mainstream measurement at any highway segment, say  $j$ , between every two consecutive unmeasured ramps. Again, the corresponding flow, namely  $q_j$ , can be obtained by fixed flow sensors, and the corresponding density be computed as

$$\rho_j = \frac{q_j}{v_j}, \quad (13)$$

where  $v_j$  is the speed of segment  $j$ , as reported by connected vehicles, and be used as a system output.

In summary, the measured outputs associated with (8)–(11) are the density (or, equivalently, the flow) at the exit of the considered highway stretch and at one highway segment between every two consecutive ramps whose flows are not measured. Therefore,

$$y(k) = Cx(k), \quad (14)$$

where  $C \in \mathbb{R}^{(l_r+l_s) \times (N+l_r+l_s)}$  is defined as

$$C = \begin{cases} c_{ij} = 1, & \text{for all } i = 1, \dots, l_r + l_s - 1 \text{ and some } n_i^* \leq j \leq n_{i+1}^* - 1 \\ c_{ij} = 1, & \text{if } i = l_r + l_s \text{ and } j = N \\ c_{ij} = 0, & \text{otherwise} \end{cases}, \quad (15)$$

where  $\bar{L}^* = \{n_1^*, n_2^*, \dots, n_{l_r+l_s}^*\}$  is the set  $\bar{L}$  ordered by  $<$ .

Although it is physically intuitive that the system described in (8)–(11), (14) and (15) is observable, the related detailed proof for certain cases, such as, for example, when a fixed sensor is placed on the mainstream at every segment immediately before an unmeasured ramp, can be found in Bekiaris-Liberis et al. (2016).

We summarize below the measurement requirements for the proposed estimation algorithm.

- The average speed of all vehicles at a segment of the highway equals the average speed of connected vehicles at the same segment, and hence, it can be obtained from regularly received messages by connected vehicles and employed by the estimator.
- The flow of vehicles at the entry of the considered highway stretch,  $q_0$ , is available via a fixed flow sensor.
- The flow at the exit of the considered highway stretch,  $q_N$ , as well as additional mainstream flow measurements  $q_j$ , where  $j$  corresponds to any highway segment between two consecutive unmeasured ramps, are available via corresponding fixed flow sensors.

### 2.2.2. Kalman filter

We utilize a Kalman filter, see, e.g., Anderson and Moore (1979), in order to estimate the traffic state of the network. Defining

$$\hat{x} = (\hat{\rho}_1, \dots, \hat{\rho}_N, \hat{\theta}_1, \dots, \hat{\theta}_{l_r+l_s})^T, \quad (16)$$

as the system state estimate, the filter equations are (see, e.g., Anderson and Moore (1979))

$$\hat{x}(k+1) = A(v(k))\hat{x}(k) + Bu(k) + A(v(k))K(k)(z(k) - C\hat{x}(k)) \quad (17)$$

$$K(k) = P(k)C^T (CP(k)C^T + R)^{-1} \quad (18)$$

$$P(k+1) = A(v(k))(I - K(k)C)P(k)A(v(k))^T + Q, \quad (19)$$

where the measurement  $z$  is a noisy version of  $y$ , and  $Q = Q^T > 0, R = R^T > 0$  are tuning parameters. In the ideal case in which there is additive, zero-mean Gaussian white noise in the state and output equations,  $Q$  and  $R$  represent the covariance matrices of the process and measurement noise, respectively. The initial conditions of the filter described by (17)–(19) are

$$\hat{x}(k_0) = \mu \quad (20)$$

$$P(k_0) = H, \quad (21)$$

where  $\mu$  and  $H = H^T > 0$ , in the ideal case in which  $x(k_0)$  is a Gaussian random variable, represent the mean and auto covariance matrix of  $x(k_0)$ , respectively.

## 3. Microscopic simulation setup for testing the proposed traffic estimation methodology

In order to thoroughly examine the effectiveness, sensitivity and further aspects of the estimation scheme described in Section 2.2 in a microscopic environment, the microscopic traffic simulation software Aimsun by Transport Simulation Systems (Transport Simulation Systems, 2014) is employed. In particular, we exploit the features provided by Aimsun API and microSDK, to extract data and results of the simulation or configure the simulation parameters and vehicle models. The default car-following model implemented by Aimsun is Gipps model (Gipps, 1981, 1986), which is used to model the dynamics of conventional and connected vehicles without ACC capabilities. The setup of the microscopic simulation-based testing of the proposed estimation methodology is shown in Fig. 1. Upstream demand and on-ramp flow data are fed to the microscopic model along with certain parameters; based on which the model produces the evolving traffic conditions for the employed scenarios. Specific traffic measurements are produced via realistically emulated detection procedures and are provided to the Kalman filter, whose parameters have been appropriately tuned; the Kalman filter then estimates the desired traffic quantities, namely  $\rho_i$  and  $\theta_i$ , which may be confronted to the “ground truth” of the simulator.

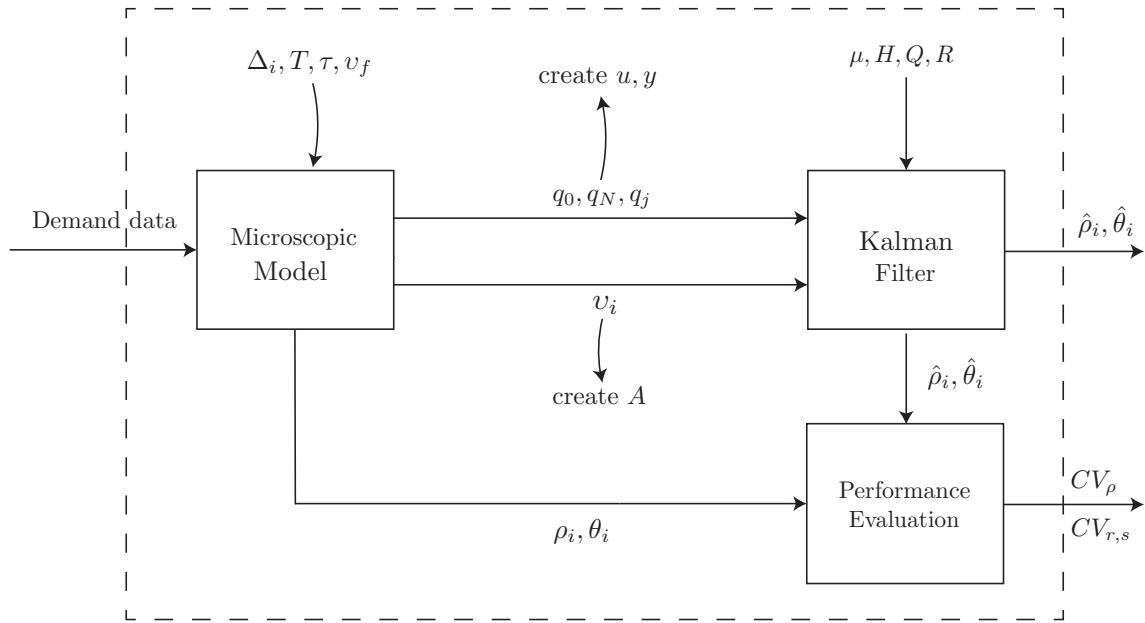


Fig. 1. Setup of the microscopic simulation-based testing environment for the proposed estimation methodology.

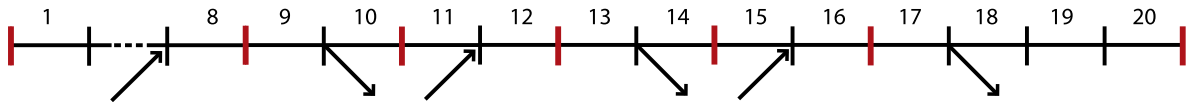


Fig. 2. The highway stretch used in the experiment. Red vertical lines indicate fixed flow sensors positioned at the network entry and exit, as well as at the end of segments between subsequent unmeasured ramps. (For interpretation of the references to color in this figure legend, the reader is referred to the web version of this article.)

### 3.1. Traffic network configuration

For the evaluation of the estimation procedure, a highway stretch of 10 km is utilized, as shown in Fig. 2. The stretch has 3 lanes and is divided into 20 homogenous segments. Three on-ramps and three off-ramps are positioned at segments 8, 12, 16 and 10, 14, 18, respectively; acceleration lanes at on-ramp locations and deceleration lanes at off-ramp locations are 100 m in length. The utilized network parameters are summarized in Table 1.

### 3.2. Employed scenario

For the purpose of testing the estimation scheme in free-flow as well as congested traffic conditions, we employ a 3-h simulation horizon, setting the simulation step as well as the reaction time of all vehicles  $\tau$  at 1 s. Inflows at the network entrance and at on-ramps are the product of an exponential distribution, with a specified mean value. The inflow at the network entrance  $q_0$  is chosen, on average, as trapezoidal. The on-ramps at segments 8 and 16 feature, on average, a constant flow of 600 veh/h for the whole simulation time; whereas the on-ramp flow at segment 12 is also on average trapezoidal. We show the demand profiles in Fig. 3. Turning rates at each off-ramp are constant at 10% of the mainstream flow of the corresponding segment.

Table 1  
Network parameter values.

Network length (km)	Number of segments N	Number of lanes	Segment length $\Delta_i$ (km)	Free speed $v_f$ (km/h)
10	20	3	0.5	120

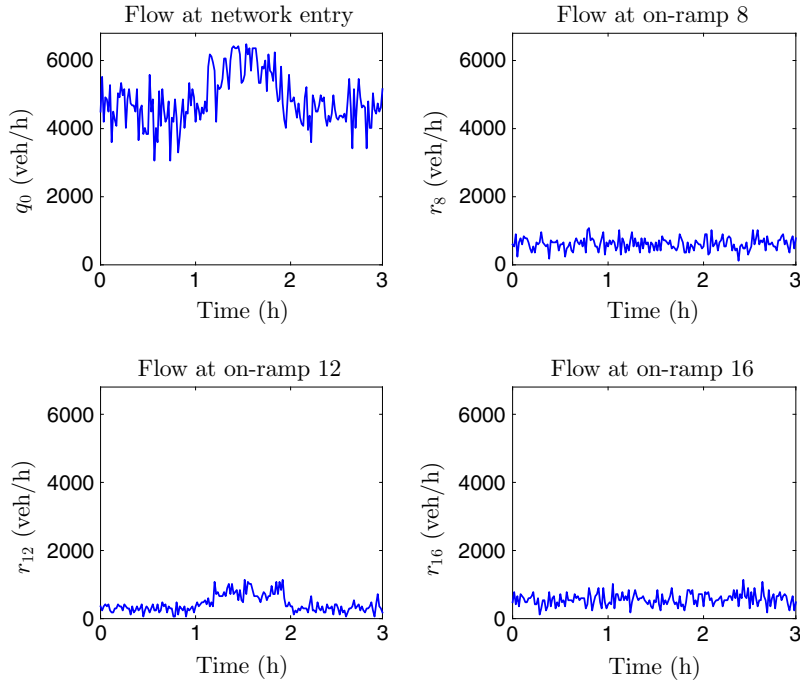


Fig. 3. The inflow at the entry of the highway stretch and the on-ramp flows at segments 8, 12, and 16.

### 3.3. Measurement configuration

We consider a measurement step  $T = 10$  s, which corresponds to the detection interval of flow sensors, as well as the interval for calculating average segment speeds.

#### 3.3.1. Flow measurements

A conventional spot sensor is placed at the entrance of the network, providing measurements of inflow  $q_0$ ; additional spot sensors are placed at the exit of the network as well as at segments 8, 10, 12, 14, and 16 (in order to guarantee observability, see Bekiaris-Liberis et al. (2016)), providing measurements of the flows  $q_{20}$ ,  $q_8$ ,  $q_{10}$ ,  $q_{12}$ ,  $q_{14}$ , and  $q_{16}$ , respectively. All flows are computed by counting the number of vehicles that cross the corresponding detector within the time interval  $(kT, (k+1)T]$ .

#### 3.3.2. Speed measurements

Segment speeds are derived from reports of a sub-population of vehicles that are connected and hence, have the ability to report their position and instant speed to the central authority at a specific frequency. In order to simulate a realistic scenario, “asynchronous” reports are considered, that is, vehicles report their speeds at different frequencies. This is implemented as follows. Upon entering the network, connected vehicles are assigned randomly a reporting frequency  $f$ , taken from a uniform distribution over the interval  $[0.1, 1]$  Hz. This way, at every simulation step (1 s), only a portion of connected vehicles report their instant speed, depending on their reporting frequency. Eventually, all individual instant speed reports of connected vehicles from each segment within time interval  $((k-1)T, kT]$  are averaged arithmetically and provide the average segment speed at time  $kT$ , namely,  $v_i(k)$ . Note that individual reports are considered as distinct measurements regardless of the vehicle that is reporting. This way, within an interval of  $T = 10$  s, a vehicle that reports every 1 s, supplies the central authority with more measurements than a vehicle that reports every 9 s, thus contributing more in the calculation of the corresponding average segment speed.

### 3.4. Measurement errors

Since all measurements produced by the simulation are error-free, we add to all measurements a zero-mean Gaussian white measurement noise. Thus, mainstream flow measurements as well as individual vehicle speed measurements obtained from connected vehicles are affected by additive noise with a Standard Deviation (SD) shown in Table 2. Considering the speed measurement accuracy of GPS mentioned in Section 2.1.1, adding noise with an SD of 5 km/h is a realistic choice, which in fact covers the worst-case scenario. Moreover, the GPS positional error, which could potentially result in a decreased speed measurements accuracy due to an erroneous determination of the segment that a vehicle is on, is, as mentioned in Section 2.1.1, extremely small compared to the length of a segment, and thus, its effect on the estimation perfor-

**Table 2**

Measurement noise (SD) of individual vehicle speeds reported by connected vehicles and of flow gathered by mainstream flow detectors.

Noise	$\gamma_i^a$	$\gamma_i^f$
SD	500 veh/h	5 km/h

mance is deemed negligible. Note that in case the transmitting device is also connected with the vehicle's electronic system, the speed measurements can be retrieved from the tachometer, whose measurements are substantially more accurate (Zito et al., 1995) (resulting in a smaller SD of the speed measurement error). However, we choose an error that is representative of GPS devices since devices equipped with GPS (e.g., smartphones, navigation systems) seem to be the most widespread devices that enable the acquisition of speed information by the central authority (Bishop, 2005). Thus, since GPS feature larger measurement error than tachometers, we actually test the performance of the estimation in worst-case-error scenarios. As for the infrastructure-based mainstream flow sensors, an error of about 10% is reported to be realistic, see, e.g., Yue (2009). Since the average inflow is around 5000 veh/h we consider an error with an SD of 500 veh/h.

### 3.5. Ground truth generation

The ground truth in our experiments, considered for evaluating the performance of the proposed estimation scheme, is represented by the density of each segment and the ramp flows (see Section 3.3.1). A segment density  $\rho_i(k)$  is calculated by dividing the number of vehicles in a segment at time  $kT$  with the segment length (0.5 km), while ramp flows are calculated in the same way as mainstream flows. However, since flows calculated in time intervals as small as 10 s are very oscillatory, we consider a moving average of the last 6 flow measurements as ground truth. Aggregated one-minute data may also be used as ground truth without affecting the estimation performance. With respect to segment speeds, in order to assess the accuracy of speed measurements from connected vehicles, we consider as ground truth the average of instant speeds of all segment vehicles every 1 s and then obtain the average for  $T = 10$  s.

## 4. Mixed traffic estimation results in the presence of conventional and connected vehicles

### 4.1. Experimental configuration

We consider the traffic network and scenario described in Section 3 to simulate a case considering mixed traffic, comprising both conventional and connected vehicles. Within this section, the attributes of both types of vehicles, such as desired speed, maximum acceleration and deceleration etc., are given by a distribution with the same mean and SD, and as a result, their behavior is statistically identical. In this environment, we will evaluate the performance of the estimation scheme for a variety of penetration rates of connected vehicles. Currently, the penetration rate of connected vehicles is quite low, however it is expected to increase substantially in the future (Diakaki et al., 2015). To account for a variety of possible current and future traffic scenarios, we evaluate the performance of the estimation scheme for a wide range of penetration rates of connected vehicles, more specifically, 2%, 5%, 10%, 20%, and 50%. Given that the microscopic model parameters (such as demand, destination, and vehicle attributes) are stochastic, we consider 10 simulation replications for each penetration rate.

Conventional and connected vehicles have identical statistical behavior, thus the traffic conditions for different penetration rates and different replications are very similar. Fig. 4 shows the traffic conditions in the scenario with a 20% penetration rate of connected vehicles. For the first hour, the inflows at the entry of the network and at all on-ramps are low, as presented in Fig. 3, and thus, free-flow conditions prevail in the whole network. During the second hour, the flows at the network entrance and at on-ramp 12 start increasing. As a result, congestion is created at segment 12 and segment 8, which propagates upstream reaching segment 4. Mild congestion is also created in segment 16, where the third on-ramp is present. At the beginning of the third hour of the simulation, since the inflows at the network entry and at on-ramp 12 are decreased, congestion gradually dissolves, and free-flow conditions are restored until the end of the simulation time, as shown in Fig. 4.

In order to evaluate the estimation results, the following performance index, known as Coefficient of Variation (CV) of the estimated density  $\hat{\rho}_i$  with respect to the ground truth density  $\rho_i$ , is used

$$CV_\rho = \frac{\sqrt{\frac{1}{KN} \sum_{k=1}^K \sum_{i=1}^N [\hat{\rho}_i(k) - \rho_i(k)]^2}}{\frac{1}{KN} \sum_{k=1}^K \sum_{i=1}^N \rho_i(k)}. \quad (22)$$

Similarly, for the unmeasured ramp flows estimation, the CV of the estimated ramp flows  $\frac{\Delta_i}{T} \hat{\theta}_i$  (see (6)), with respect to the corresponding ground truth ramp flows  $\frac{\Delta_i}{T} \theta_i$ , is given by the following equation

$$CV_{r,s} = \frac{\sqrt{\frac{1}{K(l_r+l_s)} \sum_{k=1}^K \sum_{i=1}^{l_r+l_s} \Delta_i^2 [\hat{\theta}_i(k) - \theta_i(k)]^2}}{\frac{1}{K(l_r+l_s)} \sum_{k=1}^K \sum_{i=1}^{l_r+l_s} \Delta_i \theta_i(k)}. \quad (23)$$

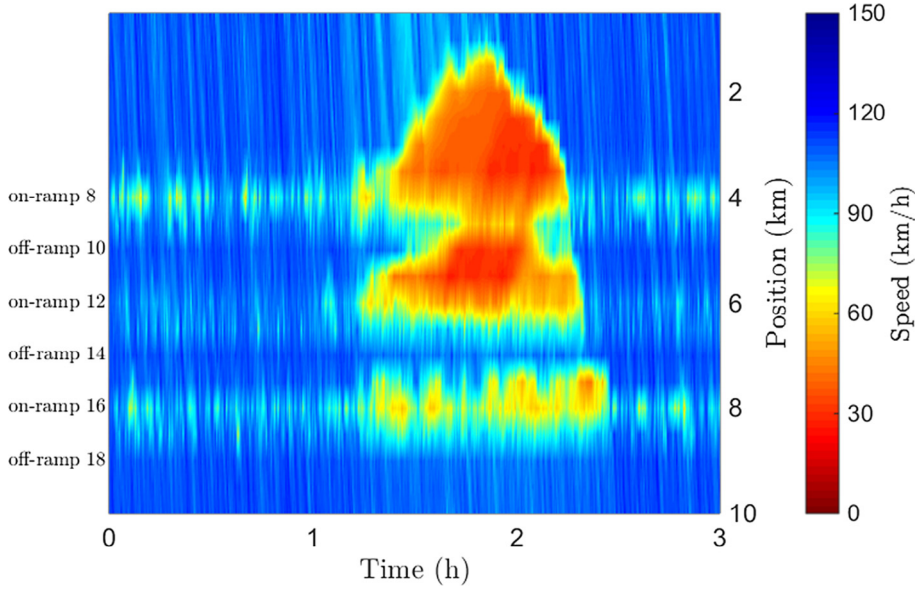


Fig. 4. Average speed of all vehicles in the employed simulation scenario of mixed traffic comprising conventional and connected vehicles.

#### 4.2. Computation of the measurements utilized by the estimator

As mentioned in Section 2.2, the estimation scheme is developed based on the assumption that the average of connected vehicles speed roughly equals the average of conventional vehicles speed. Since the driving statistics for all vehicles (connected or not) are the same, this assumption implies that the average speed of a small sample (depending on the penetration rate) of (connected) vehicles is representative for the average speed of the whole vehicle population in a segment. The accuracy of this assumption depends on the variance of individual vehicle speeds, e.g. in dependence of the average speed, see e.g., Garber and Gadirau (1989). In this section, we investigate this issue within our simulation setup in order to gain some insights on the accuracy level of the assumption above.

When calculating the average segment speed from reports by connected vehicles, two are the main problems that may degrade the estimation performance:

- For low penetration rates, when only few vehicles are present in a segment, the individual speed reports may be non-representative of the overall segment speed, due to, for example, an accidental vehicle breaking or stopping at the time of the report; or because all reports happen to originate from vehicles driving in a slow or in a fast lane, which would be lower or higher, respectively, compared to the average speed of vehicles in all lanes.
- In some cases, a low penetration rate may result in no connected vehicle being present in a segment during a time interval of  $T = 10$  s. The blue line in Fig. 5 shows the percentage of time intervals of  $T = 10$  s that feature no connected vehicle report, averaged over all segments and replications. It is evident from Fig. 5 that for penetration rates of 10% or lower a substantial percentage of time intervals are bare of reports from connected vehicles. In fact, this percentage reaches 50% for a penetration rate of 2%.

To address these problems, we feed the filter with a moving average of the available speed measurements. More specifically, for every time step  $k$ , we feed the filter with a moving average of the  $n$  latest measurements, i.e., with

$$v_i(k) = \sum_{j=0}^{n-1} \frac{v_i(k-j)}{n}, \quad (24)$$

where  $v_i(k)$  is the speed that we feed the filter at time step  $k$ , and  $v_i(k)$  is the average speed computed from connected vehicles reports at segment  $i$  and time step  $k$ . Moreover, if there are no connected vehicle reports at all at segment  $i$  during time interval  $((k-1)T, kT]$ , we take the speed  $v_i(k)$  equal to the speed reported at the previous time step, i.e.,  $v_i(k) = v_i(k-1)$ . Note that an alternative but more complex methodology for obtaining potentially more accurate measurements of the overall speed via connected vehicle reports is via application of traffic modeling as in Treiber et al. (2011), Rempe and Bogenberger (2016).

A reasonable choice for  $n$  in (24) is  $n = 6$ , since 60 s intervals are quite common for aggregation of data stemming from connected vehicles in literature, see, e.g., Rahmani et al. (2010), Lovisari et al. (in preparation). However, in our experiments,

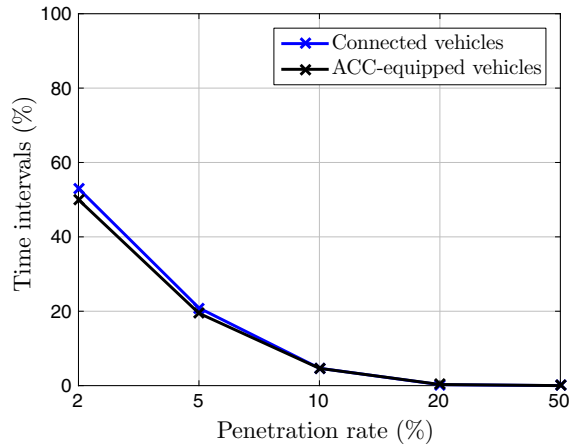


**Fig. 5.** Blue line: Average percentage of time intervals of  $T = 10$  s that feature no connected vehicle report against penetration rate of connected vehicles. Black line: Average percentage of time intervals of  $T = 10$  s that feature no ACC-equipped vehicle report against penetration rate of ACC-equipped vehicles. (For interpretation of the references to color in this figure legend, the reader is referred to the web version of this article.)

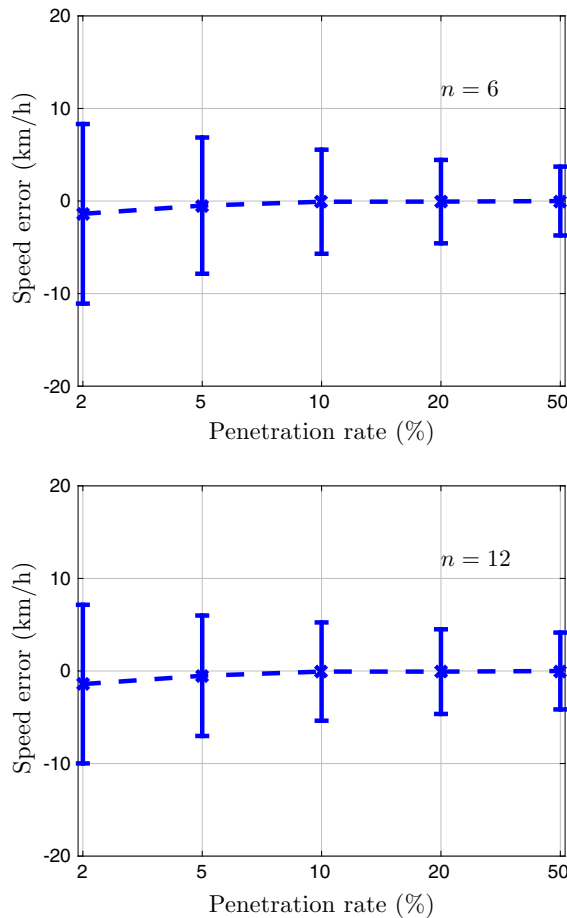
at very low penetration rates and light traffic, it is often the case that very few connected vehicles travel on a segment during 6 consecutive time intervals (i.e., 60 s). As a result, the filter may use speed measurements originating from very few (or even just one) connected vehicles, which may not be representative of the current segment speed. In order to tackle this issue, we also test a larger time window for computing the average segment speeds from connected vehicle reports, employing (24) with  $n = 12$ . In fact, a complete absence of connected vehicle reports over the last 12 time intervals is very rare in our experiments.

Fig. 6 shows the mean and SD of the error between the actual segment speed (all vehicles) and the speed that we feed the filter for both cases, i.e., when utilizing (24) with  $n = 6$  and  $n = 12$ . It can be observed that for penetration rates lower than 10%, there is a small bias in the mean error that is similar for both cases, while the SD of the error is slightly smaller for  $n = 12$ . However, for penetration rates higher than 20%, there is no bias for either of the two cases, while the SD of the error is slightly smaller for  $n = 6$ . Consequently, for low penetration rates the average speed, calculated via (24), is more representative of the overall segment speed for  $n = 12$ , whereas for higher penetration rates it is more representative for  $n = 6$ , albeit the corresponding differences are deemed minor.

#### 4.3. Selection of the estimation scheme parameters

While employing the presented estimator in practice, it is important to minimize any necessary tuning effort for the involved parameters. This will certainly be the case if the estimator performance proves little sensitive to variations of these parameters within a broad range of values. To investigate this issue, we perform a series of experiments evaluating the sensitivity of the estimation scheme to the values of the filter parameters  $Q$  and  $R$ . To this end, we consider the entry of matrix  $Q$  that corresponds to density to be equal to  $\sigma_\rho \times I_N$ , where  $I_N$  denotes the identity matrix of dimension  $N$ , whereas the entry of  $Q$  that corresponds to unmeasured ramps is considered equal to  $\sigma_{r,s} \times I_{(l_r+l_s)}$ . Similarly, matrix  $R$  is equal to  $\sigma_R \times I_{(l_r+l_s)}$ . Consequently, we compare the performance of the estimation when each of the involved parameters  $\sigma_\rho$ ,  $\sigma_{r,s}$ , and  $\sigma_R$  is varied by several orders of magnitude, while the other two remain constant. The results are shown in Fig. 7, for a variety of penetration rates of connected vehicles. It is evident in the plots that the performance of density estimation is highly insensitive to the values of the filter parameters  $\sigma_\rho$ ,  $\sigma_{r,s}$ , and  $\sigma_R$ . Ramp flow estimation is shown to be more sensitive, especially for low penetration rates of connected vehicles.

We make the following choice for the default values. We choose the parameter  $\sigma_\rho$  to be equal to 1, while  $\sigma_{r,s}$  is chosen equal to 0.03 and  $\sigma_R$  is chosen equal to 100, as shown in Table 3. Additionally, the initial values  $\mu$  that correspond to density are set equal to 15, while entries that correspond to unmeasured ramps are equal to 5; and  $H = I_{(N+l_r+l_s)}$  (see (20) and (21)); note that these initial values have some impact on the estimation results only at a short warm-up phase (when the filter is switched on), hence they are of minor significance. From Fig. 7 one can observe that this choice for the parameters  $Q$  and  $R$  results in quite low values for the performance indices for our basic scenario of 20% penetration rate of connected vehicles, as well as for all other investigated penetration rates, hence we keep the same values for  $Q$  and  $R$  throughout the paper. However, for very low penetration rates, Fig. 7 may be exploited, if one desires to obtain a better ramp flow estimation performance (since density estimation is seen to be insensitive to the choice of  $Q$  and  $R$ ) by elaborating more on the choice of the parameters  $Q$  and  $R$ . In particular, according to Fig. 7, the simple rule that for low penetration rates the value of  $\sigma_\rho$  needs to decrease, whereas the value of  $\sigma_R$  needs to increase, may be considered.



**Fig. 6.** Mean and SD of the error between actual segment speed (all vehicles) and speed utilized by the estimation scheme averaged over all segments and over 10 simulation replications against penetration rate of connected vehicles when the speed utilized by the estimator is calculated via (24) for  $n = 6$  (top) and  $n = 12$  (bottom).

#### 4.4. Performance evaluation for varying penetration rates of connected vehicles

The results of the estimation of segment densities and ramp flows for a 20% penetration rate of connected vehicles are shown in Figs. 8 and 9, respectively, when the speed fed to the filter is calculated via (24) with  $n = 6$ . It is evident from the plots that the proposed scheme successfully estimates and dynamically tracks both segment densities and ramp flows under various traffic conditions, including congested and free-flow conditions. Note also the fast convergence of the estimates towards the real values, starting from remote initial values, which were deliberately chosen far from the real values in order to test the filter's convergence properties. The segment density estimation is characterized by a performance index  $CV_\rho = 17.4\%$ , whereas ramp flow estimation is characterized by a performance index  $CV_{r,s} = 39.0\%$ . Note that we employ (22) and (23) after the initial transient period of 20 min (due to the initial estimation error) to ensure that this warm-up period is excluded from the computation of the performance indices.

The performance indices of the estimation when the speed utilized by the filter is calculated via (24) with  $n = 6$  and with  $n = 12$  are shown in Fig. 10, for various penetration rates of connected vehicles. In the first case, the filter can estimate segment densities with a satisfactory performance even for penetration rates as low as 2%. For unmeasured ramp flows the results for penetration rates of 5% or lower are less satisfactory. In the second case, the utilization of the longer moving average improves the estimated segment densities as well as the unmeasured ramp flows, more evidently for penetration rates of 5% or lower. These results are in accordance with Fig. 6.

In order to further investigate and demonstrate the specific contribution of the developed Kalman filtering (KF) approach, we also developed a less systematic, but still thoughtful and reasonable, ad hoc estimation scheme to be used as a baseline for comparison. The baseline ad hoc estimator has the same data requirements and is based on similar modeling assumptions as the KF approach, albeit without the inherent quality properties provided by the Kalman Filter. Specifically, for the ad hoc estimator, we subdivide the freeway into homogeneous parts  $j = 1, 2, \dots$ , where each part comprises all segments included between two ramps. We call these freeway parts "homogeneous" because they include no ramps that would alter

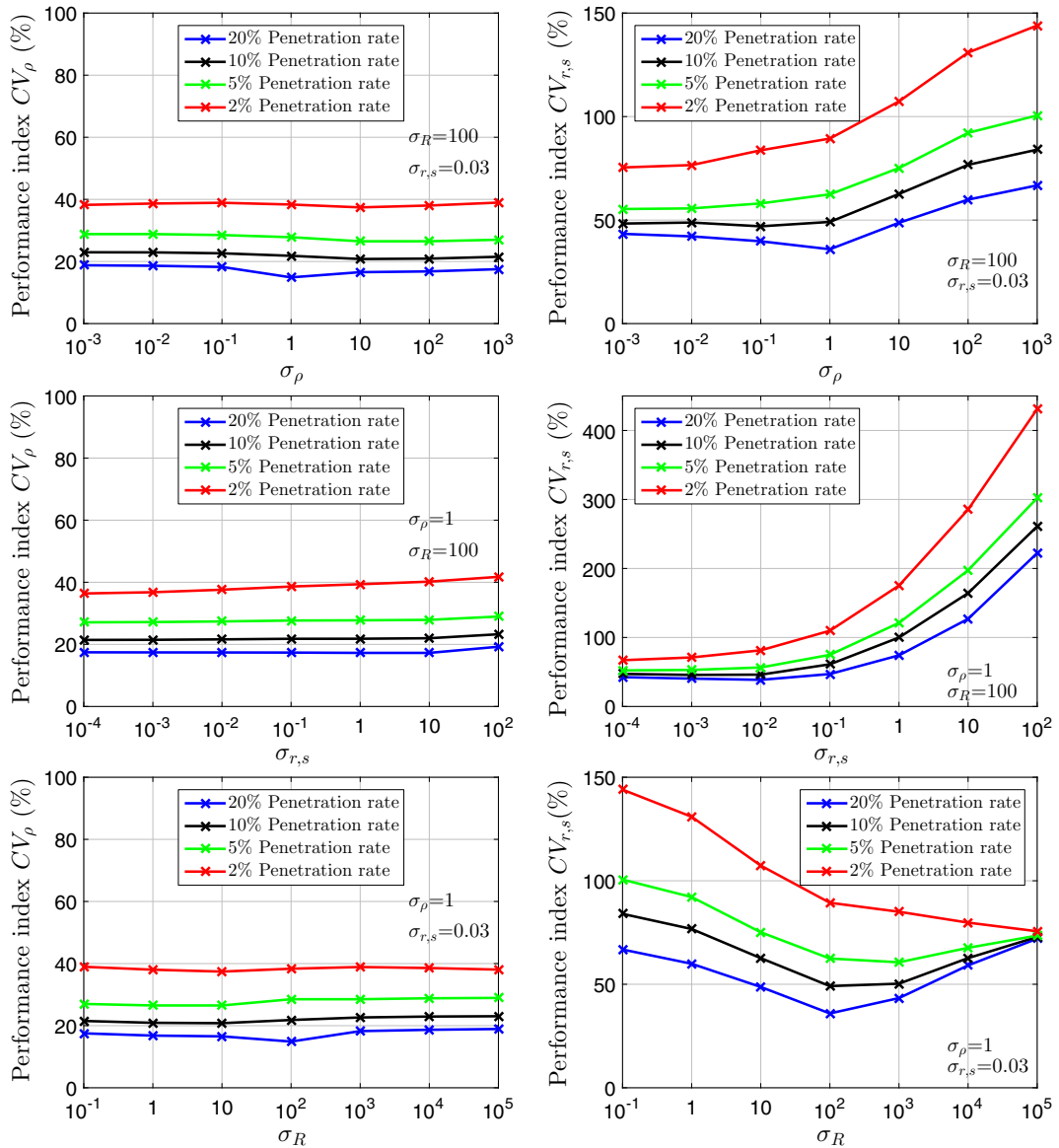


**Fig. 7.** Performance comparison of the density and ramp flow estimations for different values of the parameters  $\sigma_\rho$  (top),  $\sigma_{r,s}$  (middle), and  $\sigma_R$  (bottom), for various penetration rates of connected vehicles, when the speed utilized by the estimator is calculated via (24) with  $n = 6$ .

**Table 3**

Filter parameters used in the simulation.

$Q$	$\sigma_\rho$	$\sigma_{r,s}$	$H$
$\text{diag}(\sigma_\rho \times I_N, \sigma_{r,s} \times I_{(l_r+l_s)})$	1	0.03	$I_{(N+l_r+l_s)}$
$R$	$\sigma_R$		$\mu$
$\text{diag}(\sigma_R \times I_{(l_r+l_s)})$	100		$(15, \dots, 15, 5, \dots, 5)^T$

systematically the traffic conditions in the included segments. Thus, referring to Fig. 2, part 1 comprises segments 1–7, part 2 comprises segments 8 and 9, and so forth. For each freeway part  $j$ , we compute in real time one single corresponding average speed  $v_j$  utilizing connected vehicle reports in the same way it is also calculated for the KF estimator. Thus, the average speed  $v_j$  is computed by averaging all speed reports from connected vehicles which are located within each homogeneous freeway part  $j$ . Using this speed and the available fixed-detector-measured total mainstream flow  $q_j$  of the same freeway part, we may derive a density estimate for each freeway part  $j$  (i.e. for all its segments) from  $\rho_j = \frac{q_j}{v_j}$ .

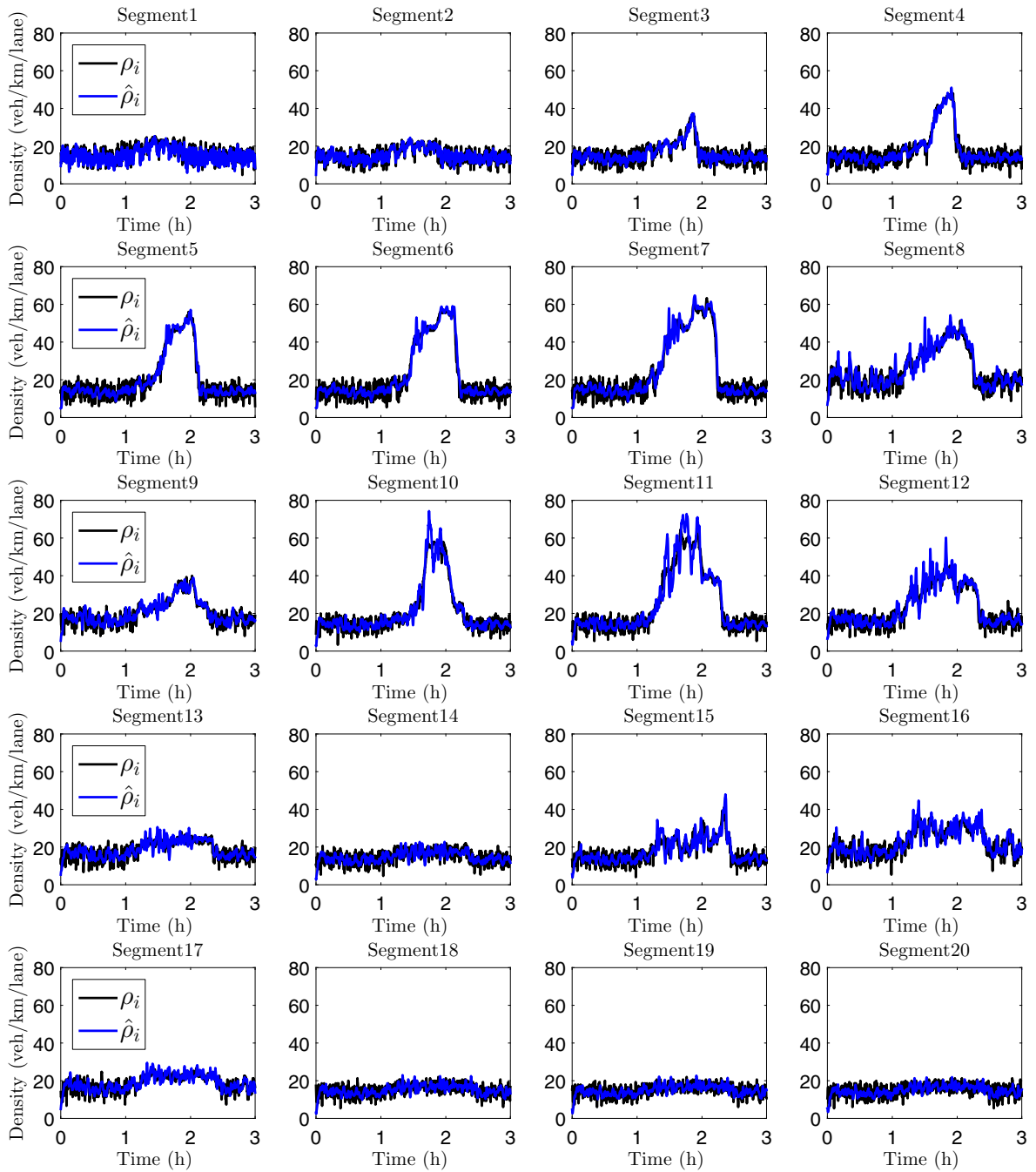


**Fig. 8.** Comparison between real (black line) and estimated (blue line) density per lane in veh/km for all network segments for mixed traffic with a 20% penetration rate of connected vehicles. (For interpretation of the references to color in this figure legend, the reader is referred to the web version of this article.)

**Fig. 11** compares the density estimation performances of the KF estimator and the ad hoc baseline scheme. It may be seen that the KF estimator achieves clearly better density estimation performance at all penetration rates, particularly as the penetration rate increases, where the improvement becomes all the more significant. In addition, for the baseline scheme, it is not clear how one could also be enabled to estimate unmeasured on-ramp or off-ramp flows, as it is done with the KF scheme. Also, the ad hoc estimator does not allow for exploitation of additional on-ramp or off-ramp flow measurements, in cases where such measurements might be available, to improve the density estimation accuracy. In summary, the baseline estimator is indeed less accurate, less general and less flexible than the proposed systematic KF-based estimation scheme.

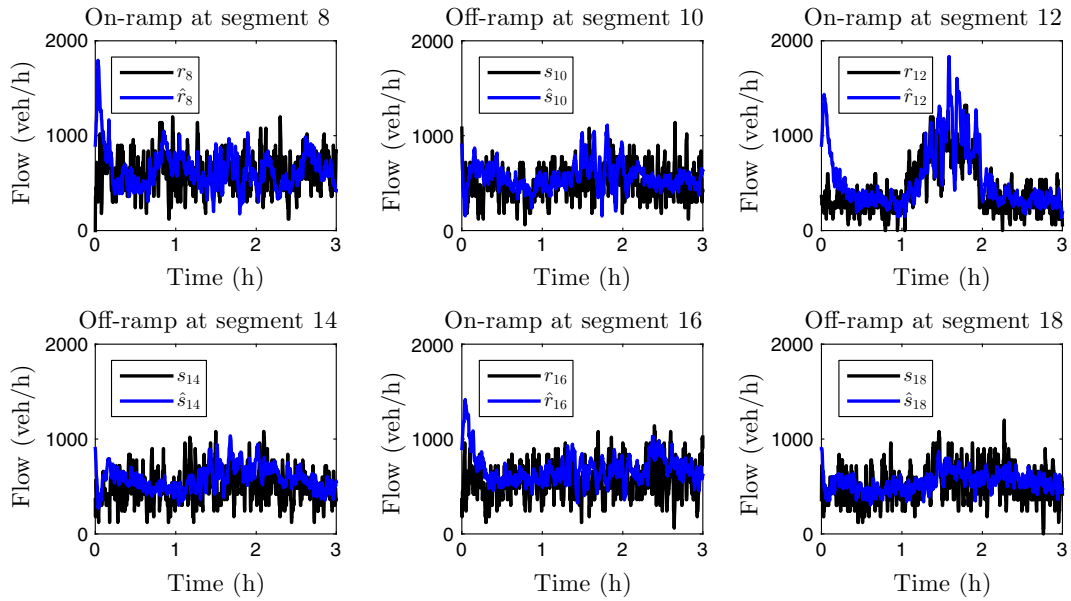


**Fig. 9.** Comparison between real (black line) and estimated (blue line) ramp flow in veh/h for all network on-ramps and off-ramps for mixed traffic with a 20% penetration rate of connected vehicles. (For interpretation of the references to color in this figure legend, the reader is referred to the web version of this article.)

## 5. Mixed traffic estimation results in the presence of conventional and ACC-equipped vehicles

### 5.1. Model of the ACC-equipped vehicles

In this section, in order to further evaluate the performance of the proposed estimation scheme under more heterogeneous conditions, we consider a scenario of mixed traffic comprising conventional vehicles and connected vehicles equipped with an ACC system. ACC-equipped connected vehicles can communicate data to the central authority concerning their state, but feature a different car-following behavior than conventional vehicles. Thus, we evaluate the performance of our estimation scheme not only when data, gathered from the central authority, stem from a small fraction of the total vehicle population, but also when these connected vehicles behave differently than conventional vehicles.

For our experiments, ACC-equipped vehicles are characterized by a different car-following model than the one used for conventional vehicles. While the default car-following model implemented in Aimsun is the Gipps model (Gipps, 1981, 1986), we consider the following Constant Time-Gap (CTG) model for an ACC-equipped vehicle  $i$ , used in Rajamani et al. (2005), similar to the one proposed by Liang and Peng (1999),

$$\ddot{x}_i = K_1(x_{i-1} - x_i - L_{i-1} - h_d \dot{x}_i) + K_2(\dot{x}_{i-1} - \dot{x}_i), \quad (25)$$

where index  $i - 1$  refers to the vehicle preceding vehicle  $i$ ;  $x_i$ ,  $\dot{x}_i$ , and  $\ddot{x}_i$  are the position, speed, and acceleration of vehicle  $i$ , respectively;  $L_i$  is the length of vehicle  $i$ ;  $h_d$  is the desired time-headway; and  $K_1, K_2$  are control gains. Moreover, the acceleration  $\ddot{x}$  is restricted between  $d_i$  and  $\alpha_i$ , which are the maximum deceleration and acceleration of vehicle  $i$ , respectively. In addition, when the speed of vehicle  $i$  computed based on (25) surpasses a certain threshold, say  $V_i^*$ , then it is set equal to this maximum speed. The values for the parameters of the model described by (25) are given in the next section.

### 5.2. Experimental configuration

We consider the scenario described in Section 3. The control gains are set at the values proposed by Liang and Peng (1999), namely  $K_1 = 1.12$  and  $K_2 = 1.70$ . Moreover, the time headway  $h_d$  is chosen in the lower side of the typical range (Kesting et al., 2007), randomly set for each ACC vehicle, according to a bounded, between 0.5 and 2 s, normal distribution with a mean of 0.8 s and an SD of 0.2 s. Finally, we set the simulation step equal to 0.2 s.

Since ACC-equipped vehicles feature a different behavior than conventional vehicles and, as mentioned in Section 1, a substantial percentage of ACC-equipped vehicles affects directly the traffic dynamics, different traffic conditions are expected in a scenario with mixed traffic comprising conventional and ACC-equipped vehicles than in the case of conventional and connected vehicles discussed in Section 4. As in Section 4, we evaluate the performance of the estimation scheme for a variety of penetration rates of ACC-equipped vehicles and consider 10 simulation replications for each penetration rate. Fig. 12 shows the traffic conditions created for a 20% penetration rate of ACC-equipped vehicles. Comparing Fig. 12 with

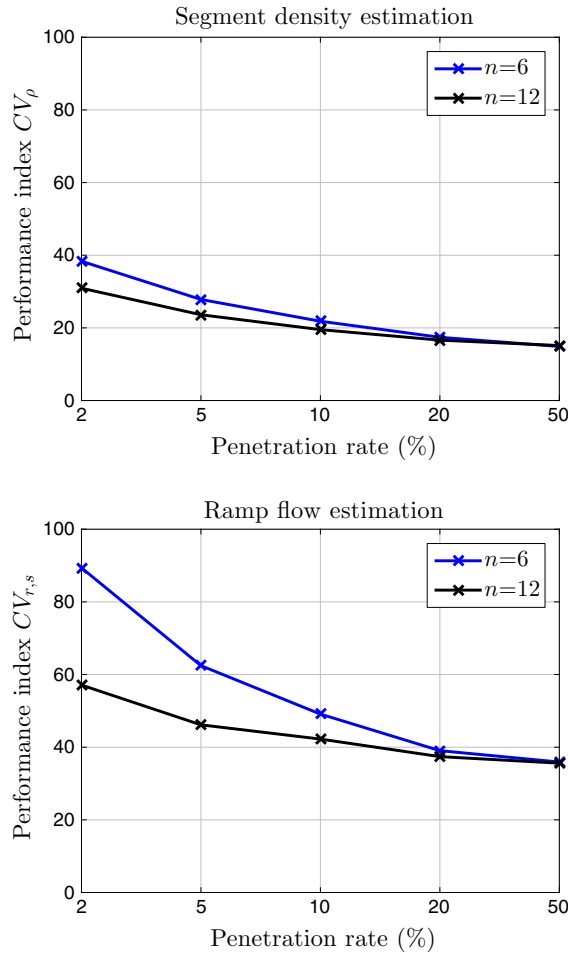


Fig. 10. Performance indices of density estimation  $CV_\rho$  (top) calculated via (22) and ramp flow estimation  $CV_{r,s}$  (bottom) calculated via (23) for various penetration rates of connected vehicles, when the speed fed to the filter is calculated via (24) with  $n = 6$  and  $n = 12$ .

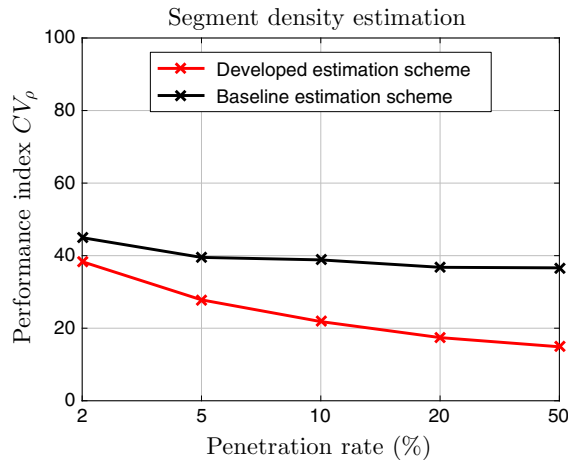


Fig. 11. Performance comparison of density estimation between the developed estimation scheme and the baseline estimation scheme for various penetration rates of connected vehicles when the speed utilized is calculated via (24) with  $n = 6$ .

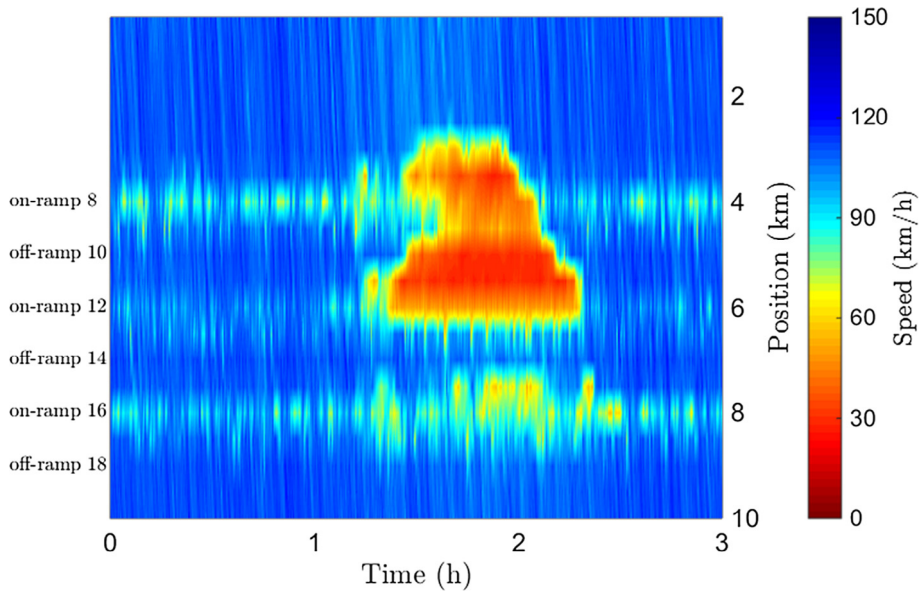


Fig. 12. Average speed of all vehicles in the employed simulation scenario of mixed traffic comprising conventional and ACC-equipped vehicles.

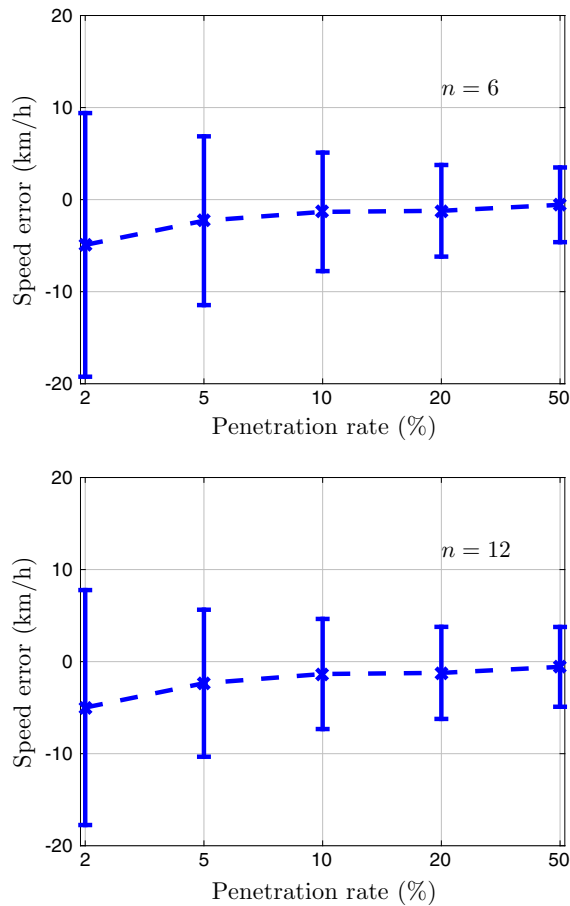
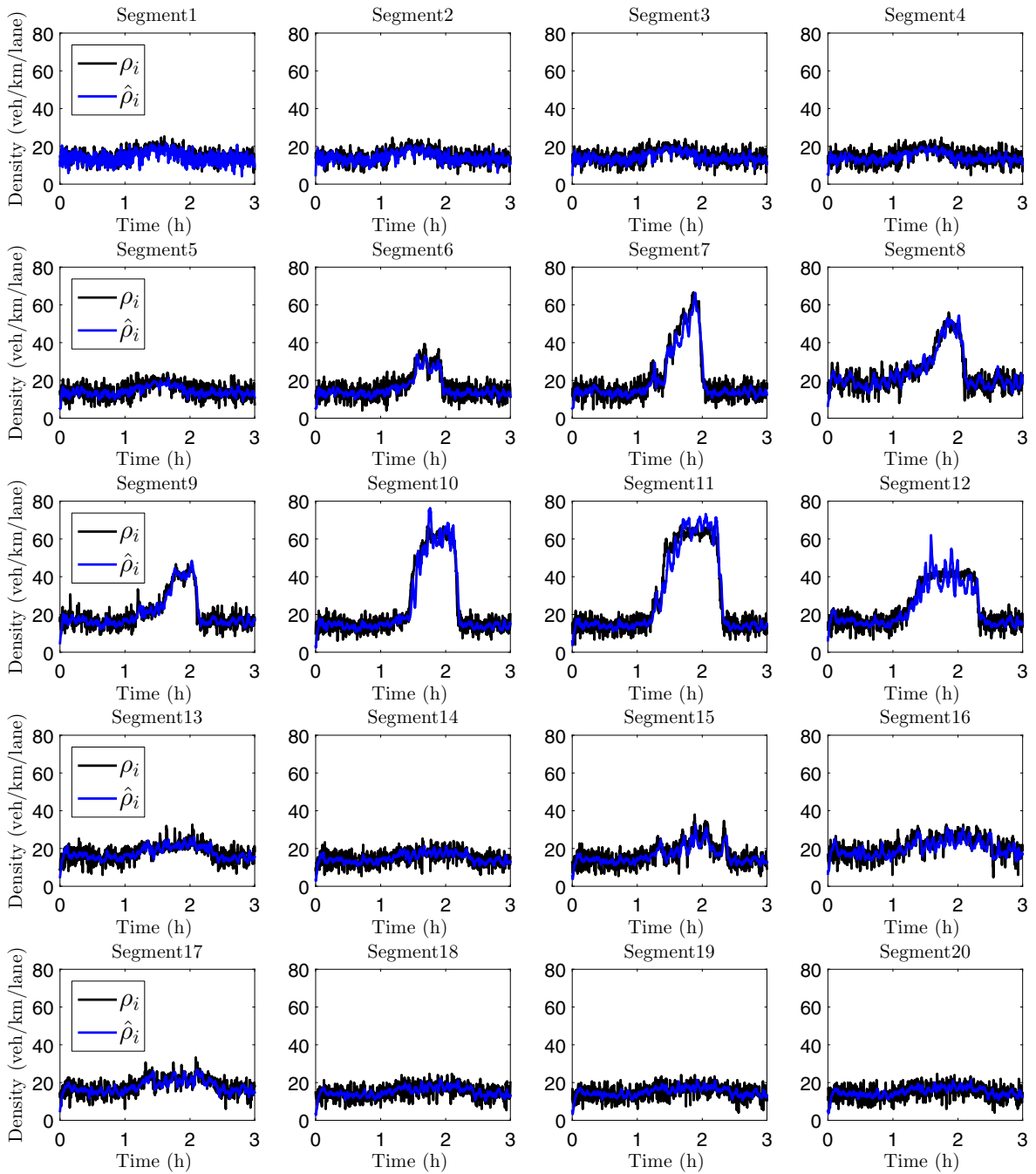


Fig. 13. Mean and SD of the error between actual segment speed (all vehicles) and speed utilized by the estimation scheme averaged over all segments and over 10 simulation replications against penetration rate of ACC-equipped vehicles when the speed utilized by the estimator is calculated via (24) for  $n = 6$  (top) and  $n = 12$  (bottom).



**Fig. 14.** Comparison between real (black line) and estimated (blue line) densities in veh/km/lane for all network segments for mixed traffic with a 20% penetration rate of ACC-equipped vehicles. (For interpretation of the references to color in this figure legend, the reader is referred to the web version of this article.)

Fig. 4, one can see that, due to the presence of ACC-equipped vehicles, congestion is milder than with conventional vehicles only. In this case, congestion is created during the second hour of the simulation, at segments 12 and 8, where the first two on-ramps are located, and propagates upstream reaching segment 6. At the location of the third on-ramp, i.e., at segment 16, some reduction of speed is observed, but without a severe congestion being evident. Halfway through the third hour of the simulation, after the inflows at the network entry and at on-ramp 12 are decreased, free flow conditions are restored until the end of the simulation time.

### 5.3. Computation of the measurements utilized by the estimator

As explained in Section 4.2, the developed estimation scheme is based on the assumption that the average connected vehicles speed roughly equals the average conventional vehicles speed. However, since the behavior of ACC-equipped vehicles differs from the behavior of conventional vehicles, we need to re-examine the accuracy of this assumption for the case of mixed traffic comprising ACC-equipped and conventional vehicles. Similar issues as in the case of regular connected vehicles described in Section 4.2, appear also when calculating the average segment speed from reports of ACC-equipped vehicles. Besides the problem of no ACC-equipped vehicle being present in a segment during a time interval of  $T = 10$  s in cases of low penetration rates, the different behavior between the two types of vehicles also increases the inaccuracy in the computation of the average segment speed. The black line in Fig. 5 shows the percentage of time intervals of  $T = 10$  s that feature no ACC-equipped vehicle report, averaged over all segments and replications. The results are very similar with the conventional connected vehicles case, showing that for penetration rates of 10% or lower a substantial percentage of time intervals are bare of reports from ACC-equipped vehicles. Consequently, we need to employ (24) for computing the speed that is utilized by the estimator.

Fig. 13 shows the mean and SD of the error between the actual segment speed (all vehicles) and the speed that we feed the filter for the case of mixed traffic featuring conventional and ACC-equipped vehicles when utilizing (24) with  $n = 6$  and  $n = 12$ . It is evident in the plots that for penetration rates lower than 10% there is a bias in the mean error that is similar for both cases, while the SD of the error is smaller for  $n = 12$ . For penetration rates higher than 20%, there is a smaller bias for both cases, while the SD of the error is slightly smaller for  $n = 6$ . The results exhibit a similar pattern with the conventional connected vehicles case, however, both the bias and SD of the error are larger in the ACC-equipped vehicles case, indicating that the speed that we feed the filter is less representative of the overall segment speed than in the connected vehicles case.

### 5.4. Performance evaluation for varying penetration rates of ACC-equipped vehicles

We consider the same values for the filter parameters as in the case of regular connected vehicles, which are shown in Table 3. Moreover, we employ (24) with  $n = 12$  for the speed utilized by the estimator, since, as shown in Fig. 13, the speed calculated with  $n = 12$  is more representative of the overall segment speed for most penetration rates. The results of the segment densities estimation for a penetration rate of 20% of ACC-equipped connected vehicles are shown in Fig. 14, while results of ramp flows estimation are shown in Fig. 15. The estimation results appear accurate for segment densities as well as ramp flows, with resulting performance indices equal to  $CV_\rho = 19.1\%$  and  $CV_{r,s} = 42.3\%$ , respectively. Performance indices of the estimation for various penetration rates are shown in Fig. 16. The results of density and ramp flow estimation are satisfactory for penetration rates of 5% or higher, whereas the estimation results are fair for penetration rates lower than 5%.

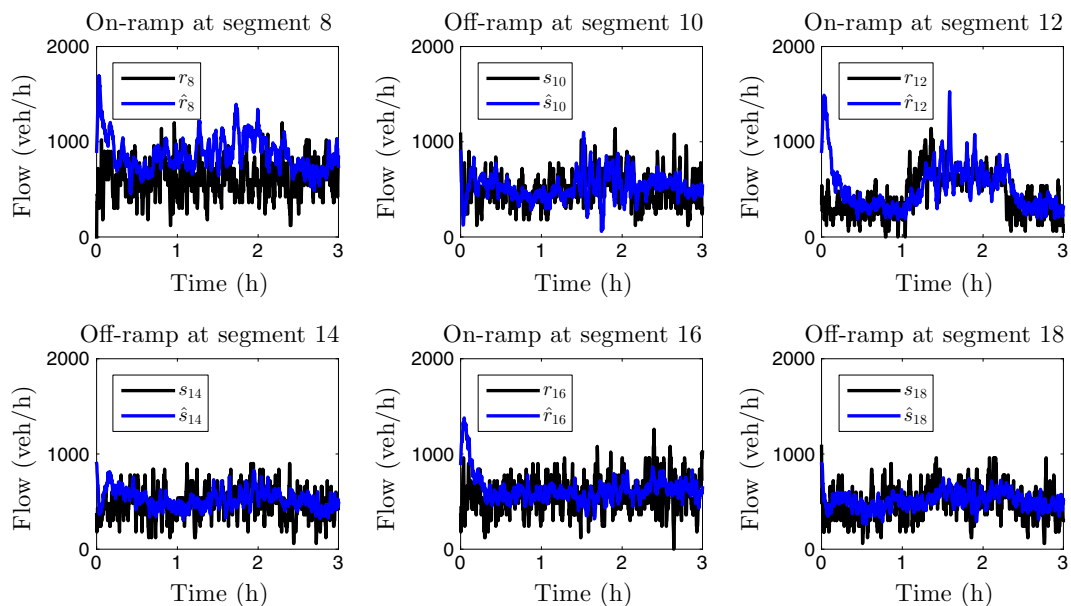
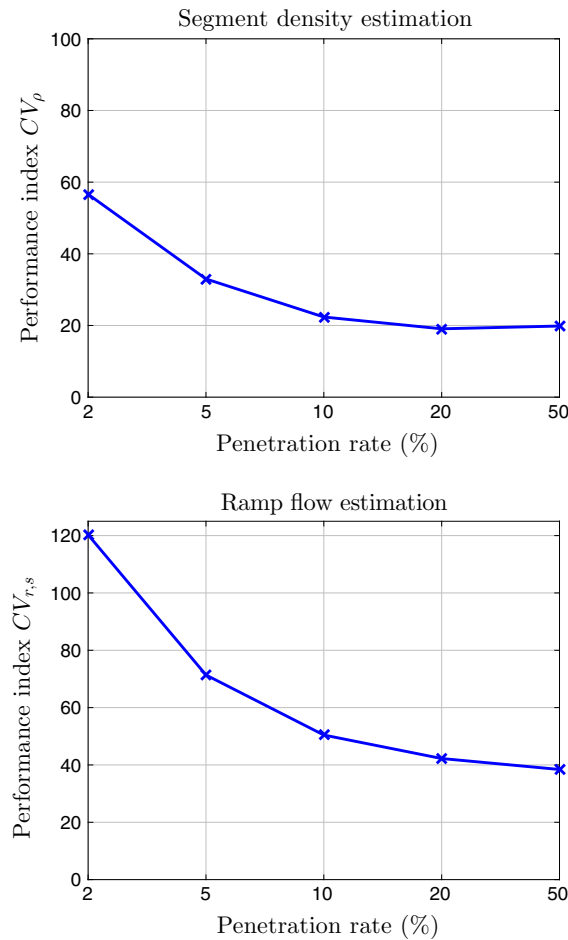


Fig. 15. Comparison between real (black line) and estimated (blue line) ramp flows in veh/h for all network ramps for mixed traffic with a 20% penetration rate of ACC-equipped vehicles. (For interpretation of the references to color in this figure legend, the reader is referred to the web version of this article.)



**Fig. 16.** Performance indices of density estimation  $CV_\rho$  (top) calculated via (22) and ramp flow estimation  $CV_{r,s}$  (bottom) calculated via (23) for varying penetration rates of ACC-equipped vehicles when the speed fed to the filter is calculated via (24) with  $n = 12$ .

### 5.5. Performance evaluation for varying penetration rates of ACC-equipped vehicles with a look-ahead speed feature

In this section we test the performance of the proposed estimation scheme in the case of mixed traffic comprising conventional and ACC-equipped vehicles when ACC-equipped vehicles report to the central authority the speed of the preceding vehicle besides their own. As mentioned in Section 2.1.2, ACC-equipped vehicles are capable of acquiring the speed and position of the preceding vehicle via on-board sensors with a range of up to 200 m (Abou-Jaoude, 2003). To this end, we implement a system in which, whenever an ACC-equipped vehicle reports its location and speed to the central authority, it also reports the speed of the preceding vehicle, if the distance of the latter is lower than 200 m and the preceding vehicle is not reporting its own speed at the same time. In reality, this may be achieved by the central authority, which can identify the duplicate information from the two vehicles by matching their position and discard the unnecessary report.

We consider the traffic network and scenario used in Section 5.4 and we simulate 10 replications for each penetration rate when ACC-equipped vehicles feature extended speed reports. Remarkably, the performance of the estimation when ACC-equipped vehicles feature extended reports is found to be virtually identical to the performance of the estimation when ACC-equipped vehicles feature normal reports, as in Fig. 16.

This can be explained by the fact that the speed of the preceding vehicle is typically very similar to the ACC-equipped vehicle's speed (thus no new speed information is provided) because, in most of the simulation experiments, ACC-equipped vehicles are able to track the speed of the preceding vehicle, maintaining a specific time-gap between the two vehicles, with a high precision (although, in general, tracking performance may depend on the parameters of the ACC model, the specific ACC law, possible actuator delays, etc.). Moreover, in cases where there are no ACC-equipped vehicles passing through a segment for a specific time interval, the problem of the lack of information remains regardless of the look-ahead feature, and thus, there is no improvement in the estimation performance.

## 6. Conclusions

The estimation scheme proposed in Bekiaris-Liberis et al. (2016) has been thoroughly tested in a microscopic simulation platform using the traffic simulator Aimsun of TSS (Transport Simulation Systems, 2014). A highway stretch that contains on-ramps and off-ramps and features a dynamic inflow demand has been employed for testing the estimation performance in both congested and free-flow conditions for varying penetration rates of connected vehicles, in two different scenarios. In the first scenario, conventional and connected vehicles have statistically identical car-following behavior; whereas in the second scenario the connected vehicles are ACC-equipped and feature a different car-following behavior than conventional vehicles. In both cases the proposed scheme has proven effective in estimating segment densities and ramp flows for various penetration rates of connected vehicles. More specifically, in the case of conventionally-driven connected vehicles, density estimation is very satisfactory for penetration rates as low as 2%, while ramp flow estimation is very satisfactory for penetration rates of 5% or higher, but fair even at lower penetrations. In the case of ACC-equipped connected vehicles with strongly different longitudinal behavior compared to conventional vehicles, density estimation is very satisfactory for penetration rates of 5% or higher, but fair even at lower penetrations; while ramp flow is very satisfactory for penetration rates of 10% or higher, but fair even at lower penetrations. Moreover, an additional scenario, where ACC-equipped vehicles can also report the speed of the preceding vehicle, has been tested. The results have shown that this addition does not improve the estimation performance.

Finally, the density estimation performance was demonstrated to be quite insensitive to the choice of the filter parameters, whereas ramp flow estimation was more sensitive. The former indicates that no serious fine-tuning effort will be required in field applications where priority is given to the availability of density estimates.

The proposed estimation scheme has several advantages for possible future real-world applications, including its simplicity, the use of a limited amount of fixed sensors, and the use of connected vehicles data, which constitute a growing source of real-time traffic information. Our current research focuses on the development of a multi-lane estimation scheme for per-lane density estimation, which may provide more detailed information about highway traffic conditions. Future research includes real-data as well as microscopic simulation-based testing of the performance of the proposed estimation scheme when it is combined with the alternative estimation scheme presented in Bekiaris-Liberis et al. (2016) or with the speed estimation scheme from Rempe and Bogenberger (2016) (aiming at achieving better overall estimation performance).

## Acknowledgement

The research leading to these results has been conducted in the frame of the project TRAMAN21, which has received funding from the European Research Council under the European Union's Seventh Framework Programme (FP/2007-2013)/ERC Advanced Grant Agreement n. 321132.

## References

- Abou-Jaoude, R., 2003. ACC radar sensor technology, test requirements, and test solutions. *IEEE Trans. Intell. Transp. Syst.* 4 (3), 115–122.
- Alvarez-Icaza, L., Munoz, L., Sun, X., Horowitz, R., 2004. Adaptive observer for traffic density estimation. *IEEE American Control Conference*, vol. 3, pp. 2705–2710.
- Anderson, B., Moore, J., 1979. *Optimal Filtering*. Prentice-Hall, Englewood Cliffs, New Jersey.
- Bar-Gera, H., 2007. Evaluation of a cellular phone-based system for measurements of traffic speeds and travel times: a case study from Israel. *Transp. Res. Part C: Emerg. Technol.* 15 (15), 380–391.
- Bekiaris-Liberis, N., Roncoli, C., Papageorgiou, M., 2016. Highway traffic state estimation with mixed connected and conventional vehicles using speed measurements. *IEEE Trans. Intell. Transp. Syst.* 17 (12), 3484–3497.
- Bishop, R., 2005. *Intelligent Vehicle Technology and Trends*. Artech House Publishers, Norwood MA, USA.
- Bose, A., Ioannou, P., 2003. Mixed manual/semi-automated traffic: a macroscopic analysis. *Transp. Res. Part C: Emerg. Technol.* 11 (6), 439–462.
- Darbha, S., Rajagopal, K., 1999. Intelligent cruise control systems and traffic flow stability. *Transp. Res. Part C: Emerg. Technol.* 7 (6), 329–352.
- Dargay, J., Gatley, D., Sommer, M., 2007. Vehicle ownership and income growth, worldwide: 1960–2030. *Energy J.* 28 (4), 143–170.
- De Fabritiis, C., Ragona, R., Valenti, G., 2008. Traffic estimation and prediction based on real time floating car data. In: *IEEE Conference on Intelligent Transportation Systems*, pp. 197–203.
- Diakaki, C., Papageorgiou, M., Papamichail, I., Nikolos, I., 2015. Overview and analysis of vehicle automation and communication systems from a motorway traffic management perspective. *Transp. Res. Part A: Policy Pract.* 75, 147–165.
- Dragutinovic, N., Brookhuis, K.A., Hagenzieker, M.P., Marchau, V.A., 2005. Behavioural effects of advanced cruise control use: a meta-analytic approach. *Eur. J. Transp. Infrastruct. Res.* 5 (4), 267–280.
- Garber, N.J., Gadirau, R., 1989. Factors affecting speed variance and its influence on accidents. *Transp. Res. Rec.: J. Transp. Res. Board* 1213, 64–71.
- Gayah, V., Dixit, V., 2013. Using mobile probe data and the macroscopic fundamental diagram to estimate network densities: tests using microsimulation. *Transp. Res. Rec.: J. Transp. Res. Board* 2390, 76–86.
- Ge, J.L., Orosz, G., 2014. Dynamics of connected vehicle systems with delayed acceleration feedback. *Transp. Res. Part C: Emerg. Technol.* 46, 46–64.
- Gipps, P.G., 1981. A behavioural car-following model for computer simulation. *Transp. Res. Part B: Methodol.* 15 (2), 105–111.
- Gipps, P.G., 1986. A model for the structure of lane-changing decisions. *Transp. Res. Part B: Methodol.* 20 (5), 403–414.
- Hegyi, A., Girimonte, D., Babuška, R., De Schutter, B., 2006. A comparison of filter configurations for freeway traffic state estimation. In: *IEEE Conference on Intelligent Transportation Systems*, pp. 1029–1034.
- Herrera, J.C., Work, D.B., Herring, R., Ban, X.J., Jacobson, Q., Bayen, A.M., 2010. Evaluation of traffic data obtained via GPS-enabled mobile phones: the mobile century field experiment. *Transp. Res. Part C: Emerg. Technol.* 18 (4), 568–583.
- Kesting, A., Treiber, M., Schnhof, M., Helbing, D., 2007. Extending adaptive cruise control to adaptive driving strategies. *Transp. Res. Rec.: J. Transp. Res. Board* 2000, 16–24.
- Kesting, A., Treiber, M., Schönhof, M., Helbing, D., 2008. Adaptive cruise control design for active congestion avoidance. *Transp. Res. Part C: Emerg. Technol.* 16 (6), 668–683.

- Leclercq, L., Laval, J.A., Chevallier, E., 2007. The Lagrangian coordinates and what it means for first order traffic flow models. In: *Transportation and Traffic Theory*.
- Liang, C.-Y., Peng, H., 1999. Optimal adaptive cruise control with guaranteed string stability. *Veh. Syst. Dynam.* 32 (4–5), 313–330.
- Lovisari, E., de Wit, C.C., Kibangou, A., 2015. Flow and Density Reconstruction and Optimal Sensor Placement for Road Transportation Networks. Available from: <1507.07093> (in preparation).
- Marsden, G., McDonald, M., Brackstone, M., 2001. Towards an understanding of adaptive cruise control. *Transp. Res. Part C: Emerg. Technol.* 9 (1), 33–51.
- Messelodi, S., Modena, C.M., Zanin, M., Natale, F.G.D., Granelli, F., Betterle, E., Guarise, A., 2009. Intelligent extended floating car data collection. *Expert Syst. Appl.* 36 (3, Part 1), 4213–4227.
- Mihaylova, L., Boel, R., Hegyi, A., 2007. Freeway traffic estimation within particle filtering framework. *Automatica* 43 (2), 290–300.
- Morbidi, F., Ojeda, L.L., De Wit, C.C., Bellicot, I., 2014. A new robust approach for highway traffic density estimation. In: *European Control Conference*, pp. 2575–2580.
- Muñoz, L., Sun, X., Horowitz, R., Alvarez, L., 2003. Traffic density estimation with the cell transmission model. In: *American Control Conference*, pp. 3750–3755.
- Ntosakis, I.A., Nikolos, I.K., Papageorgiou, M., 2015. On microscopic modelling of adaptive cruise control systems. In: *Transp. Res. Procedia*, pp. 111–127.
- Papageorgiou, M., Ben-Akiva, M., Bottom, J., Bovy, P., Hoogendoorn, S., Hounsell, N., Kotsialos, A., McDonald, M., 2007. ITS and traffic management. In: *Barnhart, C., Laporte, G. (Eds.), Transportation, Handbooks in Operations Research and Management Science*, vol. 14, pp. 715–774 (Chapter 11).
- Piccoli, B., Han, K., Friesz, T.L., Yao, T., Tang, J., 2015. Second-order models and traffic data from mobile sensors. *Transp. Res. Part C: Emerg. Technol.* 52, 32–56.
- Rahmani, M., Koutsopoulos, H.N., Ranganathan, A., 2010. Requirements and potential of GPS-based floating car data for traffic management: Stockholm case study. In: *IEEE Conference on Intelligent Transportation Systems*, pp. 730–735.
- Rajamani, R., Levinson, D., Michalopoulos, P., Wang, J., Santhanakrishnan, K., Zou, X., 2005. Adaptive Cruise Control System Design and its Impact on Traffic Flow. Project Report CTS 05-01. University of Minnesota, Department of Civil Engineering.
- Rajamani, R., Shladover, S., 2001. An experimental comparative study of autonomous and co-operative vehicle-follower control systems. *Transp. Res. Part C: Emerg. Technol.* 9 (1), 15–31.
- Ramezani, M., Geroliminis, N., 2012. On the estimation of arterial route travel time distribution with Markov chains. *Transp. Res. Part B* 46 (10), 1576–1590.
- Rao, B., Varaiya, P., 1994. Roadside intelligence for flow control in an intelligent vehicle and highway system. *Transp. Res. Part C: Emerg. Technol.* 2 (1), 49–72.
- Rempe, F., Bogenberger, K., 2016. A comparison of traffic estimation algorithms based on floating car data. In: *Presented at 1st Symposium on Management of Future Motorway and Urban Traffic Systems*, Chania, Greece.
- Roncoli, C., Bekiaris-Liberis, N., Papageorgiou, M., 2016. Highway traffic state estimation using speed measurements: case studies on NGSIM data and highway A20 in the Netherlands. *Transp. Res. Rec.* (in press).
- Roncoli, C., Papageorgiou, M., Papamichail, I., 2015. Traffic flow optimisation in presence of vehicle automation and communication systems Part II: optimal control for multi-lane motorways. *Transp. Res. Part C: Emerg. Technol.* 57, 260–275.
- Roncoli, C., Papamichail, I., Papageorgiou, M., 2016. Hierarchical model predictive control for multi-lane motorways in presence of vehicle automation and communication systems. *Transp. Res. Part C: Emerg. Technol.* 62, 117–132.
- Seo, T., Kusakabe, T., Asakura, Y., 2015. Estimation of flow and density using probe vehicles with spacing measurement equipment. *Transp. Res. Part C: Emerg. Technol.* 53, 134–150.
- Shladover, S., Su, D., Lu, X.-Y., 2012. Impacts of cooperative adaptive cruise control on freeway traffic flow. *Transp. Res. Rec.: J. Transp. Res. Board* 2324, 63–70.
- Transport Simulation Systems, 2014. *Aimsun 8 Dynamic Simulators Users' Manual*. Transport Simulation Systems.
- Treiber, M., Helbing, D., 2001. Microsimulations of freeway traffic including control measures. *Automatisierungstechnik Methoden und Anwendungen der Steuerungs, Regelungen und Informationstechnik* 49 (11), 478.
- Treiber, M., Kesting, A., 2013. *Traffic Flow Dynamics*. Springer, New York.
- Treiber, M., Kesting, A., Wilson, R.E., 2011. Reconstructing the traffic state by fusion of heterogeneous data. *Comput.-Aided Civ. Infrastruct. Eng.* 26 (6), 408–419.
- Turksma, S., 2000. The various uses of floating car data. In: *Conference on Road Transport Information and Control*, pp. 51–55.
- van Arem, B., van Driel, C.J., Visser, R., 2006. The impact of cooperative adaptive cruise control on traffic-flow characteristics. *IEEE Trans. Intell. Transp. Syst.* 7 (4), 429–436.
- VanderWerf, J., Shladover, S., Kourjanskaia, N., Miller, M., Krishnan, H., 2001. Modeling effects of driver control assistance systems on traffic. *Transp. Res. Rec.: J. Transp. Res. Board* 1748, 167–174.
- Varaiya, P., 1993. Smart cars on smart roads: problems of control. *IEEE Trans. Autom. Control* 38 (2), 195–207.
- Wang, M., Daamen, W., Hoogendoorn, S.P., van Arem, B., 2014. Rolling horizon control framework for driver assistance systems. Part II: cooperative sensing and cooperative control. *Transp. Res. Part C: Emerg. Technol.* 40, 290–311.
- Wang, Y., Papageorgiou, M., 2005. Real-time freeway traffic state estimation based on extended Kalman filter: a general approach. *Transp. Res. Part B: Methodol.* 39 (2), 141–167.
- Waterson, B., Box, S., 2012. Quantifying the impact of probe vehicle localisation data errors on signalised junction control. *Intell. Transp. Syst.* 6 (2), 197–203.
- Work, D.B., Tossavainen, O.-P., Blandin, S., Bayen, A.M., Iwuchukwu, T., Tracton, K., 2008. An ensemble Kalman filtering approach to highway traffic estimation using GPS enabled mobile devices. In: *IEEE Conference on Decision and Control*, pp. 5062–5068.
- Yim, Y., Cayford, R., 2001. Investigation of vehicles as probes using global positioning system and cellular phone tracking: field operational test. *California Partners for Advanced Transit and Highways*.
- Yuan, Y., Van Lint, J., Van Wageningen-Kessels, F., Hoogendoorn, S.P., 2014. Network-wide traffic state estimation using loop detector and floating car data. *J. Intell. Transp. Syst.* 18 (1), 41–50.
- Yuan, Y., Van Lint, J., Wilson, R.E., Van Wageningen-Kessels, F., Hoogendoorn, S.P., 2012. Real-time Lagrangian traffic state estimator for freeways. *IEEE Trans. Intell. Transp. Syst.* 13 (1), 59–70.
- Yue, Y., 2009. A traffic-flow parameters evaluation approach based on urban road video. *Int. J. Intell. Eng. Syst.* 2 (1), 33–39.
- Zhang, C., Yang, X., Yan, X., 2007. Methods for floating car sampling period optimization. *J. Transp. Syst. Eng. Inform. Technol.* 7 (3), 100–104.
- Zhao, W., Goodchild, A., McCormack, E., 2011. Evaluating the accuracy of spot speed data from global positioning systems for estimating truck travel speed. *Transp. Res. Rec.: J. Transp. Res. Board* 2246, 101–110.
- Zito, R., D'Este, G., Taylor, M., 1995. Global positioning systems in the time domain: how useful a tool for intelligent vehicle-highway systems? *Transp. Res. Part C: Emerg. Technol.* 3 (4), 193–209.